NASA Technical Memorandum 100080

Applications of the Navier-Stokes Equations to Wings and Complex Configurations Using a Zonal Approach

Jolen Flores

June 1988

NASA
National Aeronautics and
Space Administration

NASA Technical Memorandum 100080

Applications of the Navier-Stokes Equations to Wings and Complex Configurations Using a Zonal Approach

Jolen Flores, Ames Research Center, Moffett Field, California

June 1988

NASA
National Aeronautics and
Space Administration

Ames Research Center
Moffett Field, California 94035

SUMMARY

The simulation of a transonic viscous flow over a series of three-dimensional configurations, ranging from isolated wings to relatively complete aircraft, is presented. A fast, diagonalized Beam-Warming algorithm is used in conjunction with a zonal approach to solve the Euler/Navier-Stokes equations for these applications. The computer code, called Transonic Navier-Stokes, uses four zones for wing configurations and up to 19 zones for more complete aircraft configurations. For the inner zones adjacent to no-slip surfaces, the thin-layer Navier-Stokes equations are solved, while in the outer zones the Euler equations are solved. Numerical results are presented and compared with experiment (when available) for wing calculations and a more complete configuration based on the F-16A aircraft.

ZONAL GRID APPROACH

The zonal philosophy will be explained in detail for the four-zone wing version. First, a base grid is generated about a wing composed of NACA 0012 cross sections having a 20° leading edge sweep, an aspect ratio of 3.0, and a taper ratio of 1.0 via an elliptic-solver grid-generator.[1] Once the base grid is generated, a zoning algorithm is used to divide the grid into separate zones. Referring to figure 1, the first grid zone (grid 1) is the base grid itself, with a small block of grid points near the wing removed. The second grid zone (grid 2) basically occupies the space left open by the block of points removed from grid 1, with a small region of overlap included (usually one or two grid cells on all boundaries). Grid 2 is constructed so as to contain twice as many grid points in each spatial direction as the original base grid. This refinement of grid 2 relative to the base grid is accomplished via cubic-spline interpolation. Similar to grid 1, grid 2 has a small block of points removed near the wing.

The final two grid zones (grids 3 and 4) occupy the space left open by the block of points removed from grid 2, again with a small region of overlap included. Grids 3 and 4 are constructed so as to contain the same number of points, in both the spanwise and chordwise directions, as grid 2. However, the grid points in the normal direction are highly clustered in order to capture viscous effects on the wing surfaces. Grid 3 is designed to capture the upper wing surface viscous effects and grid 4, the lower wing surface viscous effects. The two outer inviscid grid zones are topologically represented in the computational domain as cubes, with smaller cubes removed from the middle. The third and fourth viscous zones are topologically represented as simple cubes in the computational domain. The code also has the option to model wind tunnel walls and a C_p comparison for free-air versus wind tunnel walls will be shown.

NACA 0012 WING RESULTS

The flow conditions for this test case are a free-stream Mach number of 0.826, angle of attack of 2°, and a Reynolds number of eight million based on chord. For this case the wind-tunnel-wall effects are very significant. This can be seen in figure 2 where the pressure coefficient distributions from the Transonic Navier-Stokes (TNS) code, with and without the walls modeled, are compared with experiment.[2] The shift in shock position caused by the tunnel walls is obvious. The shock position for the case with walls is in good agreement with the experimental shock position, while the free-air shock position is too far upstream

by about 10-12% of chord. This solution required about 500 iterations, at a data processing rate of 5 μs per iteration, per grid point. For the current grid, this required about 45 min of central processing unit time on the Cray XMP/48 computer using a single processor. For a more detailed explanation of the results, the reader is referred to references 3 and 4.

F-16A WING-FUSELAGE-INLET RESULTS

The modified F-16A geometry is shown in figure 3, illustrating the exclusion of the tail assembly. Note that the forebody, canopy, leading edge strake, wing, shelf regions, inlet, and diverter sections are unmodified, and represent the exact F-16A geometry. It is extremely difficult, with a single grid, to achieve appropriate viscous clustering at all solid boundaries for this complicated geometry. However, with the use of zonal methods, this becomes a manageable problem.

As with the wing code, a base grid is fed into the zonal routine, which subsequently creates 19 zones by subdividing the original base grid. This process is controlled by various parameters which exist in the zonal routine. The zones created are essentially of three types: 1) inviscid zones, 2) viscous zones with clustering on one face corresponding to wing or fuselage no-slip surfaces, and 3) viscous zones with clustering on two adjacent faces corresponding to the wing-fuselage juncture. Figure 4 shows the zoned planform and fuselage surface grids about the modified F-16A geometry. The total number of grid points is approximately 300,000. The inviscid zones away from the geometry have as few as 3000 grid points, whereas the viscous zones near the body contain as many as 28,000 grid points.

Flow-through conditions are applied at the inlet face; that is, boundary values at the inlet face are determined by extrapolation of the computed solution values from one plane upstream of the inlet face. No-slip conditions are applied on all solid surfaces including the underside of the fuselage, the diverter section, and the upper surface of the inlet.

Computational results are presented for the modified F-16A geometry for $M_\infty = 0.9$, $\alpha = 4.12°$, and a Reynolds number based on root chord of 4.5 million. Figure 5 shows a comparison of the computed pressure distribution with experiment[5] for four different spanwise stations along the wing and one station along the upper surface fuselage centerline. The data points designated by the upward- and downward-pointing triangles identify the experimental pressure distributions for the upper and lower surfaces of the wing, respectively. The solid line indicates the numerical computation. At the leading edge of the wing, the computation tends to underpredict the pressure coefficient. This underprediction is caused by the lack of grid resolution at the leading edge of the wing. The trailing edge prediction of pressure is quite good all along the span of the wing. The lower surface prediction is good, and the upper surface agreement is also good except that the aft-shock position is underpredicted by about 10% of chord. Failure to accurately pick up the aft-shock strength and position is largely due to insufficient grid resolution in the streamwise direction. The base grid used in this calculation contained 60 points on the wing in the streamwise direction.

The computed pressure distribution along the fuselage upper surface centerline (shown in the bottom of fig. 5) is in good agreement with the experimental pressures, up to the beginning of the canopy. The expansion and recompression regions caused by the canopy are underpredicted by the computation. Again, this is caused by insufficient grid resolution. Downstream of the canopy the agreement is good. The last few experimental data points reflect the tail-assembly influence, which was not simulated in the computation.

Figure 6 displays C_p comparisons between the computed solution and the experiment for two streamwise cross-sectional planes near the inlet region. Figure 6(a) shows a comparison at a streamwise location

of $\xi = 0.43$, and figure 6(b) shows a comparison at $\xi = 0.83$. The parameter ξ is aligned with the streamwise direction and is equal to 0.0 at the inlet face and 1.0 at the end of the inlet (where the inlet diverter has fully merged into the fuselage). The symbols indicate experimental results, and the solid line computed results. The dashed line indicates the cross-sectional body definition, the inlet, diverter section, and the leading edge strake. Generally the computed pressure results are in good agreement with experimental results. The sharp jump in pressure, which is exhibited in both the experimental and computational results, is caused by the expansion of flow around the strake leading edge.

This solution required about 3000 iterations, at a data processing rate of 36 μs per iteration, per grid point. For the current grid, this required about 20 hours of central processing unit time on the Cray XMP/48 computer using a single processor. References 6 and 7 give the reader a more indepth analysis of the grids, and flow results for the F-16A.

CONCLUSIONS

Transonic flow fields about wing, wing-fuselage, and wing-fuselage-inlet geometries have been computed using a zonal Euler/Navier-Stokes formulation. In the present approach the flow domain is divided into several zones or blocks. This zonal approach offers several distinct advantages over non-zonal techniques. The flow field can be broken into grid zones which tend to adapt to the flow field in a beneficial way. That is, regions of the flow field with significant gradients can be resolved with dense grid zones, while regions in which the flow has small gradients can be resolved with coarse grid zones. In addition, the use of a zonal technique makes the task of computing flow fields about complex geometries more tenable.

REFERENCES

[1] Sorenson, R. L.; and Steger, J. L.: Grid Generation in Three Dimensions by Poisson Equations with Control of Cell Size and Skewness at Boundary Surfaces, Advances in Grid Generation-FED, K. Ghia, ed., vol. 5, 1983.

[2] Lockman, W. K.; and Seegmiller, H. L.: An Experimental Investigation of the Subcritical and Supercritical Flow about a Swept Semispan Wing. NASA TM-84367, June 1983.

[3] Flores, J.; Holst, T. L.; Kaynak, U.; Gundy, K.; and Thomas, S. D.: Transonic Navier-Stokes Wing Solution Using a Zonal Approach: Part 1. Solution Methodology and Code Validation. AGARD Paper 30A, 58th Meeting of the Fluid Dynamics Panel, Symposium on Applications of Computational Fluid Dynamics in Aeronautics, Aix-en-Provence, France, April 1986.

[4] Flores, J.: Convergence Acceleration for a Three-Dimensional Euler/Navier-Stokes Zonal Approach. AIAA Paper 85-1495, July 1985.

[5] Reue, G. L.; Doberenz, M. E.; and Wilkins, D. D.: Component Aerodynamic Load from 1/9-Scale F-16A Loads Model. General Dynamics Report 16PR316, Fort Worth, Tex., May 1976.

[6] Flores, J.; Reznick, S. G.; Holst, T. L.; and Gundy, K. L.: Transonic Navier-Stokes Solutions for a Fighter-Like Configuration. AIAA Paper 87-0032, Jan. 1987.

[7] Flores, J.; Chaderjian, N. M.; and Sorenson, R. L.: Simulation of Transonic Viscous Flow over a Fighter-Like Configuration Including Inlet. AIAA Paper 87-1199, June 1987.

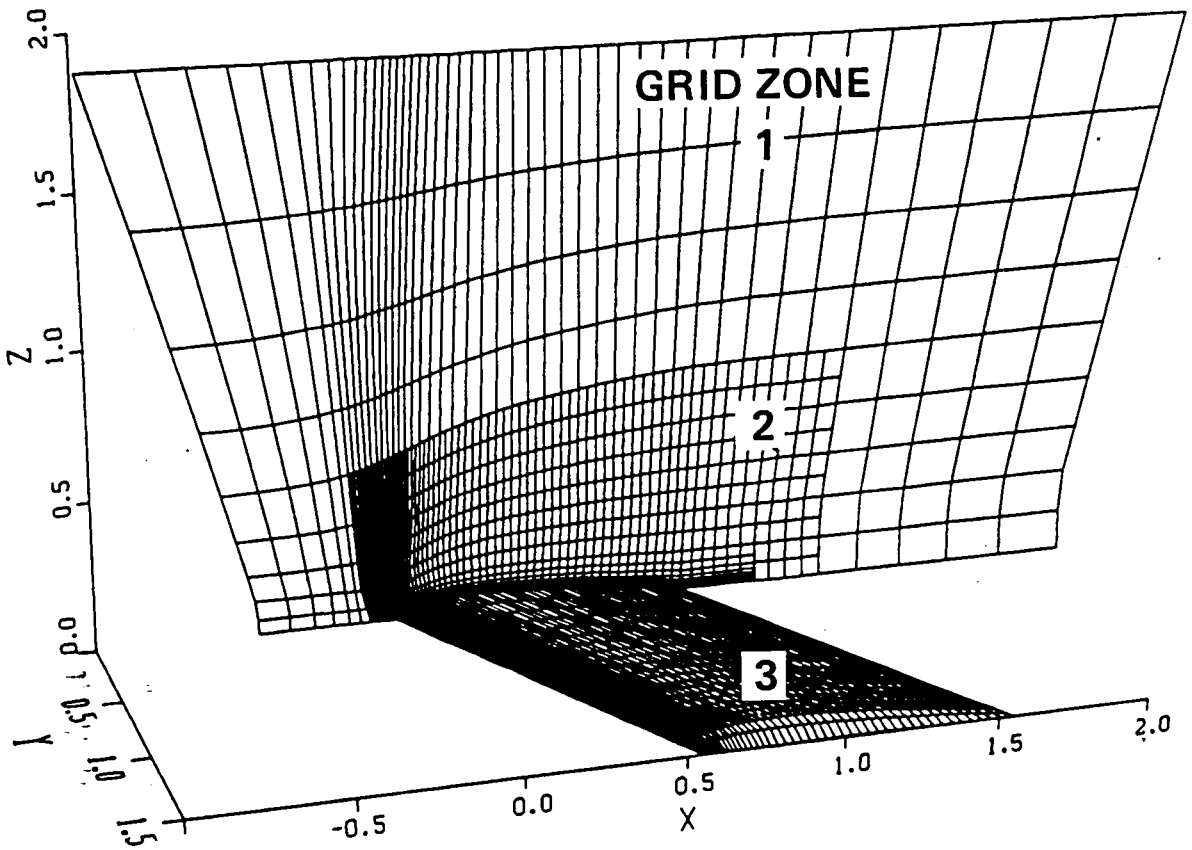

Figure 1.- Perspective view of embedded grid with upper symmetry plane ($y = 0, z \geq 0$) and wing surface highlighted.

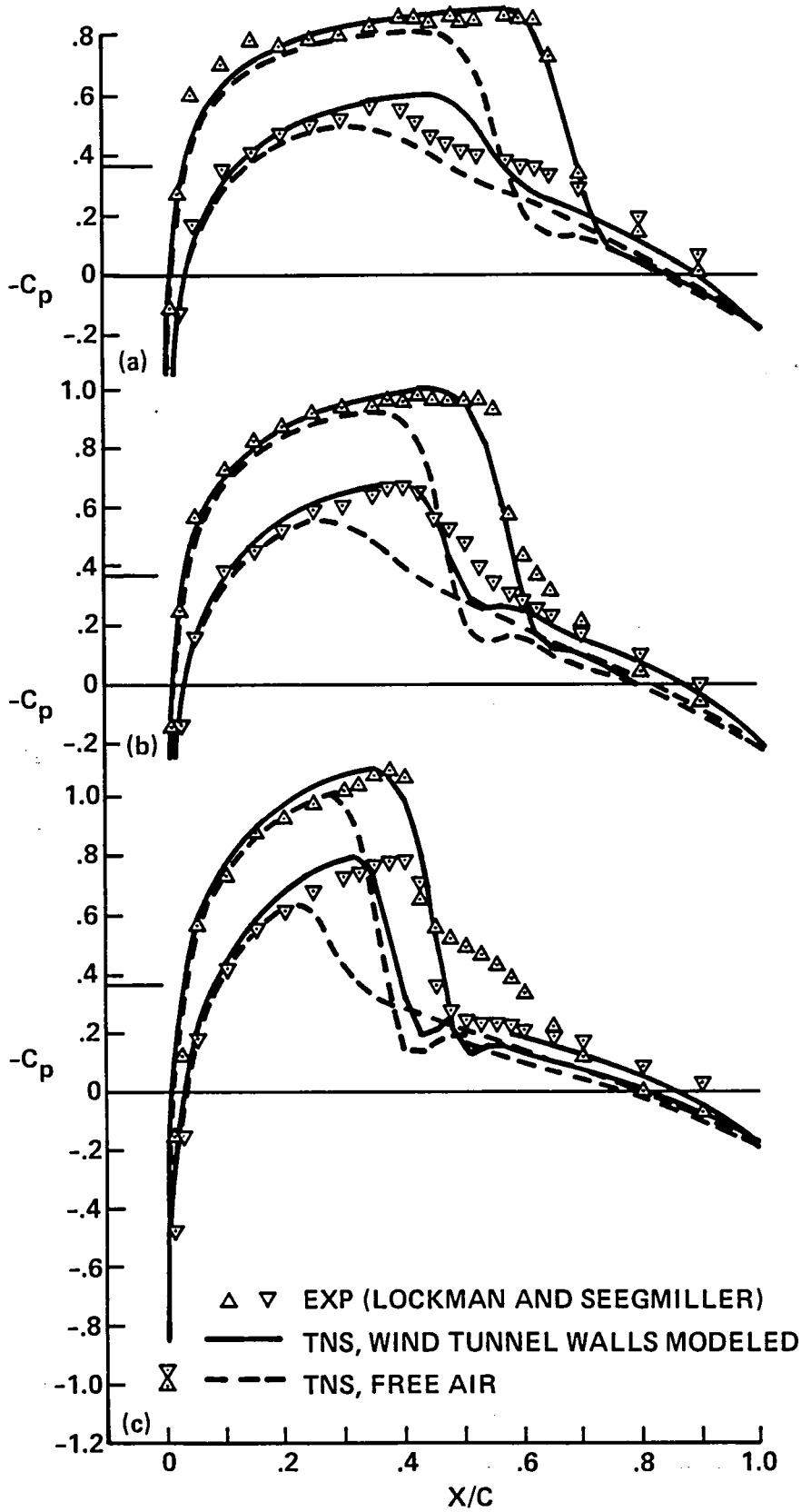

Figure 2.- Pressure coefficient comparisons; NACA 0012 airfoil sections, $\Lambda_{LE} = 20°$, $AR = 3.0$, $TR = 1.0$, $M_\infty = 0.826$, $\alpha = 2°$, $Re = 8\text{x}10^6$. a) $2y/b = 0.25$; b) $2y/b = 0.50$;

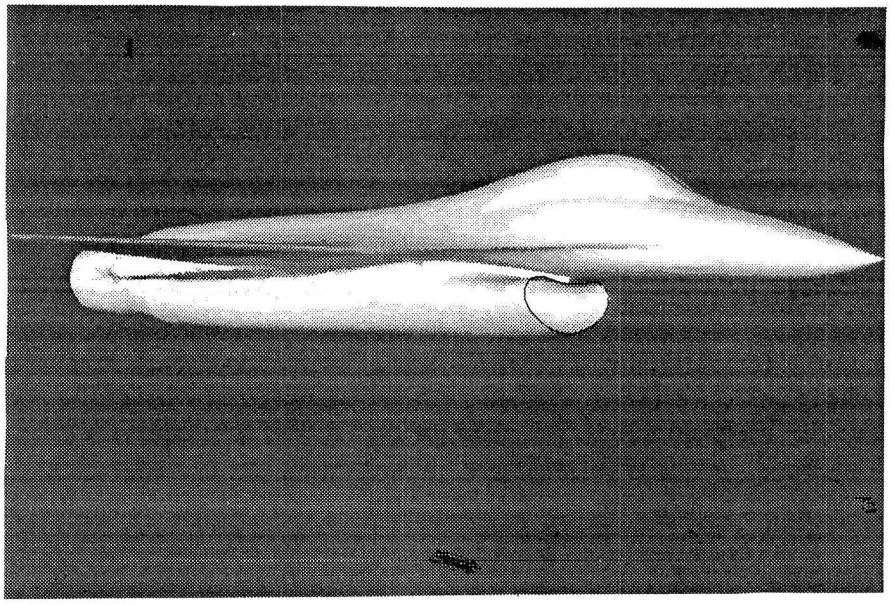

Figure 3.- Wing-fuselage-inlet geometry derived from the F-16A configuration.

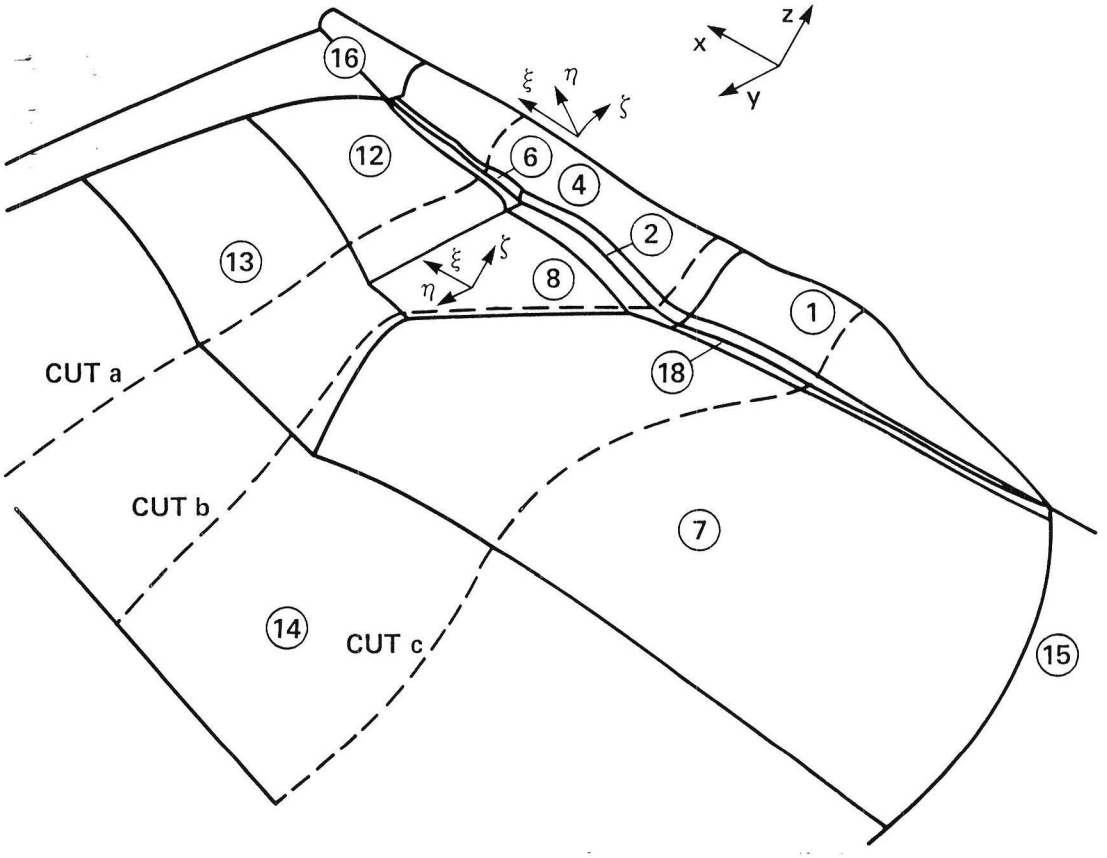

Figure 4.- Different zonal grids about the F-16A wing-fuselage geometry.

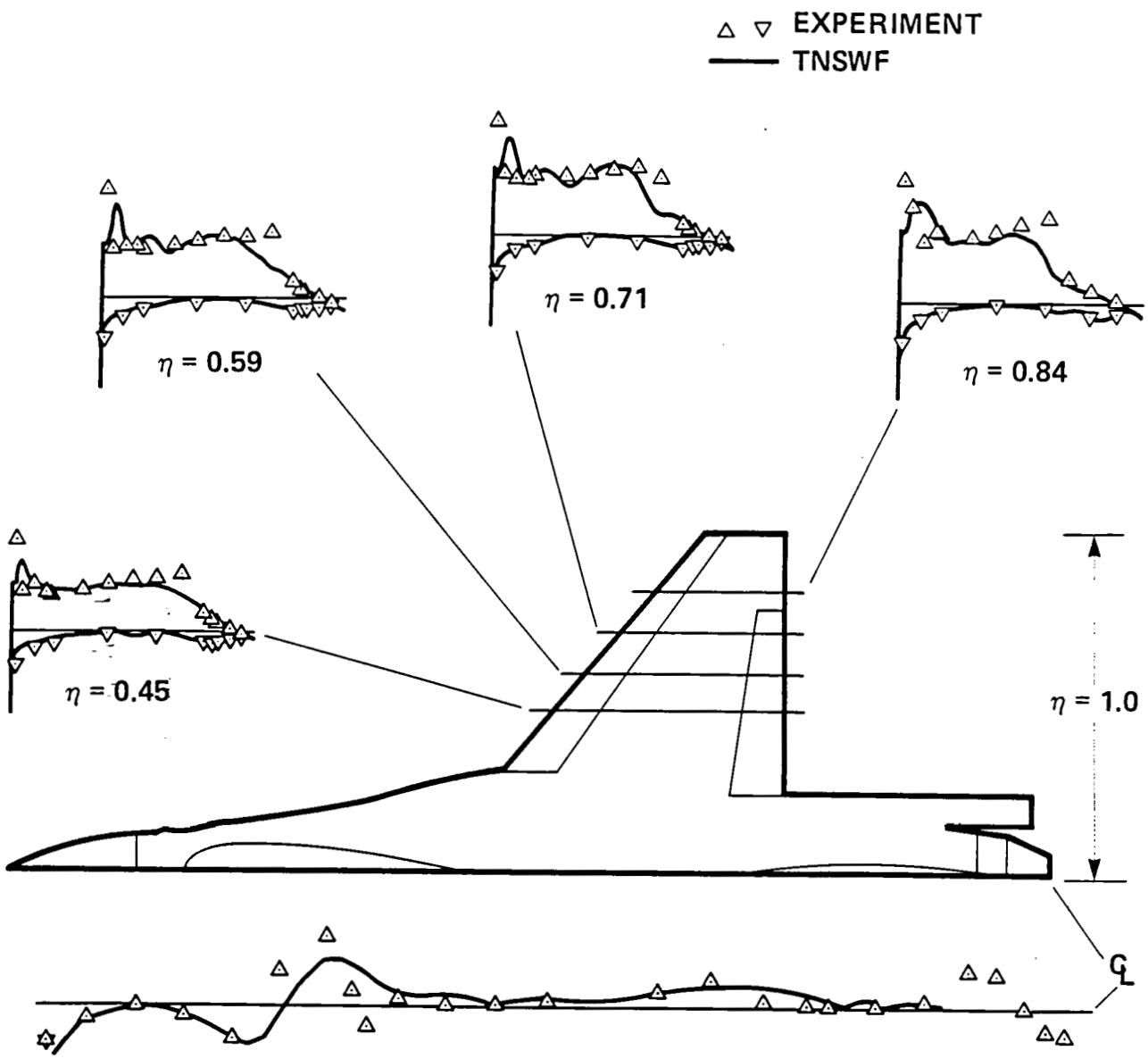

Figure 5.- Comparison of the F-16A wing-fuselage pressure coefficient distributions; $M_\infty = 0.90$, $\alpha = 4.12°$, $Re_c = 4.5\text{x}10^6$.

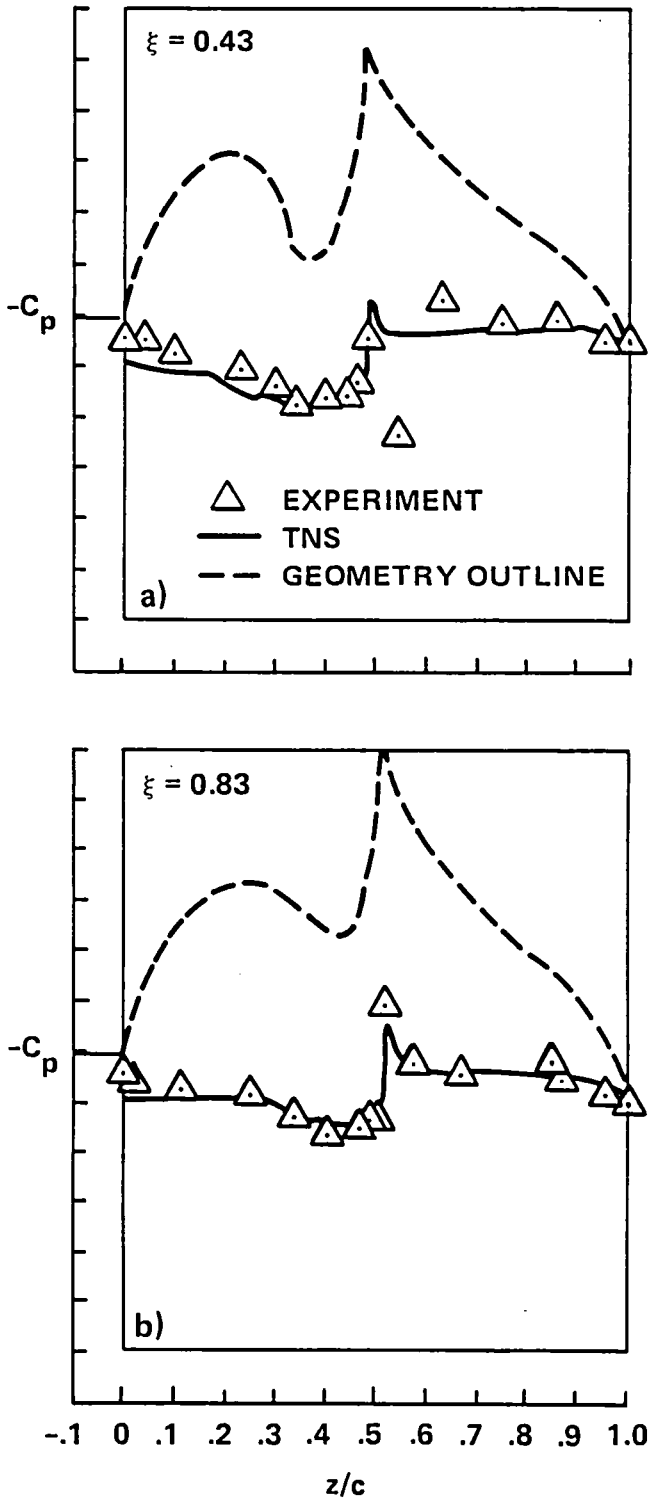

Figure 6.- Comparison of pressure coefficient distributions for the F-16A wing-fuselage-inlet configuration in the vicinity of the inlet-diverter region; $M_\infty = 0.90$, $\alpha = 4.12°$, $Re_c = 4.5 \times 10^6$. a) $\xi = 0.43$, b) $\xi = 0.83$.

NASA National Aeronautics and Space Administration

Report Documentation Page

1. Report No.	2. Government Accession No.	3. Recipient's Catalog No.
NASA TM-100080		

4. Title and Subtitle

Applications of the Navier-Stokes Equations to Wings and Complex Configurations Using a Zonal Approach

5. Report Date

June 1988

6. Performing Organization Code

7. Author(s)

Jolen Flores

8. Performing Organization Report No.

A-88115

10. Work Unit No.

505-60

9. Performing Organization Name and Address

Ames Research Center
Moffett Field, CA 94035

11. Contract or Grant No.

13. Type of Report and Period Covered

Technical Memorandum

12. Sponsoring Agency Name and Address

National Aeronautics and Space Administration
Washington, DC 20546-0001

14. Sponsoring Agency Code

15. Supplementary Notes

Point of contact: Jolen Flores, Ames Research Center, MS 258-1, Moffett Field, CA 94035
(415)694-5369 or FTS 464-5369

16. Abstract

The simulation of a transonic viscous flow over a series of three-dimensional configurations, ranging from isolated wings to relatively complete aircraft, is presented. A fast, diagonalized Beam-Warming algorithm is used in conjunction with a zonal approach to solve the Euler/Navier-Stokes equations for these applications. The computer code, called Transonic Navier-Stokes, uses four zones for wing configurations and up to 19 zones for more complete aircraft configurations. For the inner zones adjacent to no-slip surfaces, the thin-layer Navier-Stokes equations are solved, while in the outer zones the Euler equations are solved. Numerical results are presented and compared with experiment (when available) for wing calculations and a more complete configuration based on the F-16A aircraft.

17. Key Words (Suggested by Author(s))	18. Distribution Statement
Navier-Stokes Zonal approach Complex configurations	Unclassified - Unlimited Subject Category - 02

19. Security Classif. (of this report)	20. Security Classif. (of this page)	21. No. of pages	22. Price
Unclassified	Unclassified	12	A02

